Two-dimensional density distribution of metastable atoms in an inductively coupled plasma in Ar

Masahiro Tadokoro, Hajime Hirata, Nobuhiko Nakano, Zoran Lj. Petrović,* and Toshiaki Makabe
Department of Electrical Engineering, Faculty of Science and Technology, Keio University, 3-14-1 Hiyoshi, Yokohama 223-8522, Japan
(Received 29 June 1998)

A two-dimensional density distribution of metastables Ar($1s_5$) (in Paschen notation) in an inductively coupled plasma (ICP) reactor in argon, driven by one-turn radio-frequency current coil at 13.56 MHz, has been investigated by laser absorption spectroscopy. Measurements were made over a pressure range of 15–300 mTorr, and powers between 20 and 400 W. In these conditions, metastable density varied between 1×10^{10} and 2.3×10^{11} cm^{-3}. Even for the the position far from the coil, 140 mm far from the source region, metastable density remained comparatively high (of the order of 10^{10} cm^{-3}). As the power increases the metastable density drops down significantly especially for the center of the discharge where the highest electron density is anticipated. In general, the metastable profiles can be explained by combining the expected profile of efficient excitation with diffusion and with the radial dependence of the density of the electrons that can quench the metastable levels by inducing transitions to higher excited states. Therefore we have compared the data for metastable profiles with the excitation rates for one radiative level with a relatively short lifetime and with the radial dependence of electron density obtained by using a Langmuir probe. [S1063-651X(98)01612-2]

PACS number(s): 51.50.+v, 51.10+y, 52.25.Fi

I. INTRODUCTION

Inductively coupled plasma [1] (ICP) is currently being used for the manufacturing of microelectronic components as a technique of choice that can provide ultralarge scale integrated (ULSI) plasma processing for 12-in wafers with sufficient uniformity. However, details of plasma maintaining mechanisms are not all known and further work on diagnostics and modeling of such plasmas is required and is carried out with an aim to improve the next generation of plasma devices. Especially, it has been shown that the metastable molecules play a determining role in the kinetics of ICP [2–4]. This is so because the basic characteristics of ICP systems is that in the absence of capacitively coupled electrodes no high field regions develop and consequently plasma is sustained with mostly low energy electrons. Therefore stepwise processes (in particular ionization), are of increased importance [5–7]. In addition, it appears that the kinetics of metastable levels is controlled by electron induced transitions to radiative levels (quenching) making it difficult to apply simple tracer techniques, which proved to be useful in the case of argon in capacitively coupled plasmas (CCP's) [7].

The aim of this paper is to present our results on laser absorption diagnostics of an argon ICP in order to establish the density profiles of metastables. For comparison, the data obtained by Langmuir probes and optical emission spectroscopy will also be shown.

In our previous papers [2,8,9], we investigated the spatial distribution of the net excitation rate in an ICP reactor in argon under a variety of external conditions by utilizing computer-aided optical-emission tomography. Those results have shown that the stepwise excitation might be expected to have an influence on the profile of the plasma. In addition, we have studied the azimuthal anisotropies of excitation, space-time resolved excitation in argon [10] and spatial emission profiles in oxygen ICP [11]. At the same time we have taken advantage of the simple and symmetric geometry that was used for our experimental system and developed a theoretical description of the ICP that will, thanks to the simplicity of the symmetry, allow quantitative comparisons with experiment [12,13].

Under those circumstances, it is important to determine the spatial distribution of metastables, and to deduce the influence of the stepwise excitation by way of metastables on the plasma structure. As has been shown in other systems and in our studies the metastable density profiles are an important test of the theories or input into the theory [4].

There are numerous studies in the literature of the role of metastables in rf capacitively coupled discharges [7,14,6]. As for the ICP, metastable densities of buffer gas atoms have so far only been measured by Hebner [3]. He has performed a systematic study of spatial profiles of metastable densities in ICP by a laser absorption technique, using a Ti sapphire laser. His ICP had a planar five turn coil geometry. This author obtained line integrated profiles that were in one case Abel inverted to give the radial metastable number density profile with a maximum of 1.3×10^{11} cm^{-3}. In this work other $1s$ levels were studied as well with the densities of $1s_2$, $1s_3$, and $1s_4$ being a factor of 5–8 lower than the density of the $1s_5$ state and all increased with power up to a certain point (100 W), where saturation occured, while the density of the $1s_5$ state did not increase with power.

However, the geometry of field distribution for the flat coil ICP is complex and radial distributions of metastable densities have not been measured in sufficient detail required by the modeling. Having this in mind, as well as the requirement of producing data specifically for the geometry of our experiment that is open for a quantitative comparison with a relatively simple theory, we believe that the present work is fully warranted. Related studies on ICP and rf discharges in general, which take advantage of laser absorption spectros-

*Also at Institute of Physics, University of Belgrade P.O.B. 57, 11001 Belgrade, Yugoslavia.

copy and laser induced fluorescence, include studies of the profiles of metastable ions [15], laser absorption diagnostics of high-pressure ICP's for plasma light sources [16], measurements of time resolved sheath fields by the laser induced fluorescence [17], argon metastable densities in dc glow and magnetron discharges [18,19], laser collision induced fluorescence measurement of electron number density [20], and applications of laser induced fluorescence as a diagnostic tool in general [21].

II. EXPERIMENT AND PROCEDURE

The basic reaction chamber and the procedure for maintaining the plasma (see Fig. 1) are the same as used in our earlier studies of ICP [2,8]. The chamber is made of a quartz cylinder 10 cm in diameter and 20 cm high. The system is powered by a 13.56-MHz rf generator, supplying through a matching box a single turn coil, fitted closely to the quartz tube on the outside. Power to the ICP, including the matching network, is measured by an in-line wattmeter. Peak-to-peak values of the radio-frequency (rf) voltage to the coil (V_{p-p}) and currents close to the powered and the ground terminals (I_{p-p}) are monitored by a set of voltage and current probes.

We have used the gas flow of 100 sccm (standard cubic centimeter per minute) of high-purity argon. Constant pressure was maintained by a system of pumps and leak valves and measurements were performed at pressures between 15 and 300 mTorr. Gas is introduced at the top of the chamber and pumped out symmetrically at the bottom of an additional extension, eight-sided chamber (that serves the purpose for positioning the wafer for remote plasma processing) attached to the quartz cylinder. The pumping terminals are far from the coil region (16 cm) assuring uniform and symmetric flow of the gas through the coil region.

The line emission from the excited argon $3p_5$ state (in Paschen notation) was used in this paper for comparisons with laser absorption data. The optical detector was mounted on a hand of a computer-controlled, industrial, four-axis robot [2] that was able to provide enough flexibility to allow application of the computer aided tomography [9]. Absolute calibration of the measured spectrally resolved signal allowed us to determine excited state densities as a function of radial position and in this paper we use such profiles to represent the distribution of the radiative states. The complete procedure as well as the analysis were the same as in our previous papers [2,8,9] so we shall give no further details. The Langmuir probe measurements were also described earlier [8].

A. Experimental setup and analysis for the laser absorption measurements

The laser source is a solid state diode laser operating in a single mode (New Focus-6200) from 769 to 790 nm. The laser was found to be very stable over long periods of time, much longer than the duration of one measurement. The laser was mounted on a translational stage and allowed to scan along the diameter of the ICP at different distances from the coil (z). In Fig. 1(a) we show a schematic diagram of the experimental setup for laser absorption measurements.

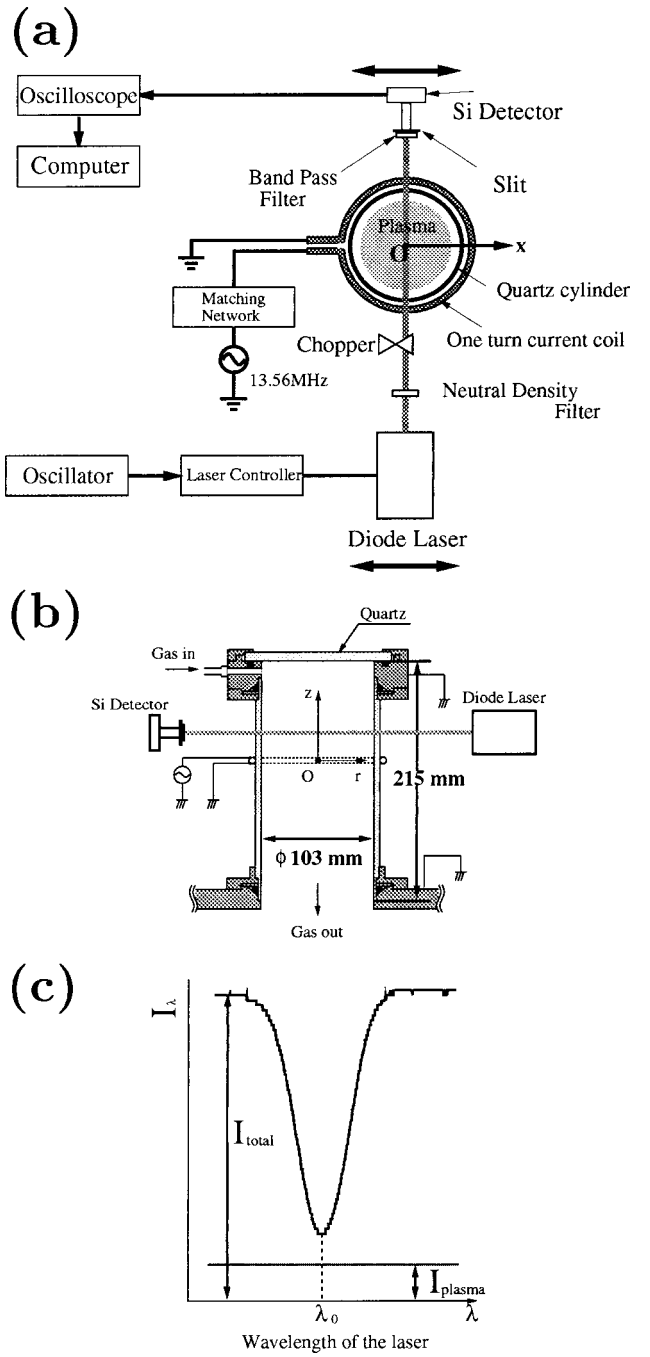

FIG. 1. Schematic diagram of the experimental apparatus, (a) the top view and (b) side view of the ICP reactor, and (c) typical recorded line profile.

The Si laser detector (Coherent-LM-2) was used to detect the intensity of the laser light. The active region of the detector was large enough to minimize any instabilities of the signal due to vibration of both the detector and the laser. A spectral bandpass filter ($\Delta\lambda = 10$ nm) and a slit were placed in front of the Si detector to reduce the emission from the plasma. The dimension of the laser beam is limited by the spatial resolution to 1×2 mm. In addition it proved necessary to attenuate the intensity of the laser light by neutral density filters down to the level of 2 μW cm^{-2} in order to avoid saturation of the signal and perturbation of plasma. The laser line width (5 MHz) is much narrower than the line

profile so it is not necessary to perform deconvolution of the profile.

The detector and filters were mounted on the same robot that was used for the optical emission scans [2,8,9]. For each position of the laser the position of the detector was adjusted to obtain the maximum signal. The spectral region was first selected manually in the region of the desired absorption line. Then the wavelength of the laser was modulated by a sawtooth signal fed into the controller providing the wavelength scans of the order of 0.015 nm. The scan was extended sufficiently to cover beyond the entire line in order to obtain accurately the background for line profile determination. The emission from plasma entering the detector was subtracted by using a chopper for the laser light. One such scan is shown in Fig. 1(c).

The laser was tuned to the 772.38 nm line corresponding to the $1s_5$-$2p_7$ transition, which was used to establish the densities of the lower metastable state $1s_5$. The laser absorption signal obtained at one position is a line integral across the plasma. Measurements were performed over the range $0 \leqslant x \leqslant 52$ mm and the Abel inversion technique for the absorption signals is employed in the same way as used for the emission signals [2,8] to determine the radial dependence of the metastable atoms. Two different techniques were used to reconstruct the radial profile, the first was a direct numerical application of the Abel inversion procedure [2] and the other consisted of doing the inversion without the numerical differentiation. The procedures were tested on a given test profile and were shown to give excellent and almost identical results, certainly within the experimental uncertainty.

The absorption signal $I(\lambda)$ observed at one point x is an integral over the length of the plasma at that point (l) [see Fig. 1(c)]:

$$I(\lambda) = I_0 \exp\left(- \int^{l} k(\lambda) dy \right), \tag{1}$$

where $k(\lambda)$ is the spectrally resolved absorption coefficient. The integral over the line profile gives

$$A(x) = \int \left(\int^{l} k(\lambda) dy \right) d\lambda = \int \ln\left(\frac{I_0}{I_{total} - I_{plasma}} \right) d\lambda . \tag{2}$$

Finally, after performing the Abel inversion of $A(x)$ to $A(r)$ the radial profile of the metastables is obtained from

$$n^*(r) = A(r) \left(l \frac{\pi e^2 \lambda_0^2}{mc^2} f \right)^{-1}, \tag{3}$$

where f is the oscillator strength, λ_0 is the transition wavelength, and other quantities have the standard meaning.

We have carried out measurements of both emission and absorption at different distances from the coil (z) [see Fig. 1(b)], the closest that we could approach it was $z = 5$ mm from its center. Apart from covering the range of approximately 50 mm on both sides of the coil we have also made measurements at $z = 140$ mm far from the coil in one direction. This measurement was made inside the octagonal auxiliary chamber attached to the ICP reactor for the purpose of studying the remote processing. The probe measurements were performed close to the coil as well, corresponding to $z = 5$ mm.

III. EXPERIMENTAL RESULTS AND DISCUSSION

Measurements of the density distribution of metastables Ar($1s_5$) were made over a pressure range of 15–300 mTorr, and powers between 20 and 400 W. Normally the flow rate of 100 sccm was used. We should also note that measurements were also performed for the other low metastable state $1s_3$ and the radial profiles were generally of the same shape as for $1s_5$ but the magnitude of the number density was up to a factor of 10 lower. This can be expected on the basis of the available quenching and cascading coefficients and is in agreement with the findings of Hebner [3,5].

A. Pressure dependence of the metastable density

The Abel inverted 2D profiles of metastable atom density are shown in Fig. 2. The profiles were recorded as a function of radial position (r) and the distance from the coil (z). Maximum density of metastables is reached for the lowest pressure covered here (15 mTorr) and the densities up to 2.3×10^{11} cm^{-3} are observed. At the highest pressure of 300 mTorr the maximum density is a factor of 4 lower but the mean density is even a factor of 10 lower. This is due to a much sharper profile at higher pressures. The radial dependencies observed here cannot be explained on the basis of simple ''diffusion versus production determined profile'' arguments [22].

First, we should bear in mind that electrons required to excite metastables must have more than 11 eV of energy. The mean free path of electrons at 300 mTorr is short and they gain such energy only in the region of a high azimuthal field. On the other hand, electron induced collisional quenching proceeds by coupling the metastables to one of the radiative states, and energies as small as 0.1 eV are required for that process [5]. Thus in the region of the center of the discharge where high field is shielded by plasma, low-energy electrons efficiently quench the metastables while there is no production due to their low energy. At low pressures electrons may have long mean free paths, sufficient for the ''nonlocal'' approximation to be valid [23]. Under those conditions electrons carry high energy obtained from the azimuthal field all the way to the center of the discharge and consequently production extends over the entire radius; it may even have a maximum at $r = 0$ [23]. One can see at the lowest pressures that the metastable profile close to the coil still maintains a caldera shaped profile indicating that our conditions still correspond to the maximum excitation close to the walls [2,8,9]. Further from the coil the production weakens but is nevertheless significant. At such low pressures diffusion of the metastables may also contribute significantly to the shape of the radial dependence of the metastable density. At high pressures the caldera profile is dominant even away from the coil. Another important feature is that the density of metastables may be constant or even increase at high z, especially for $r = 0$ (see Fig. 2). This is due to decreasing electron quenching as one moves away from the plane of the coil.

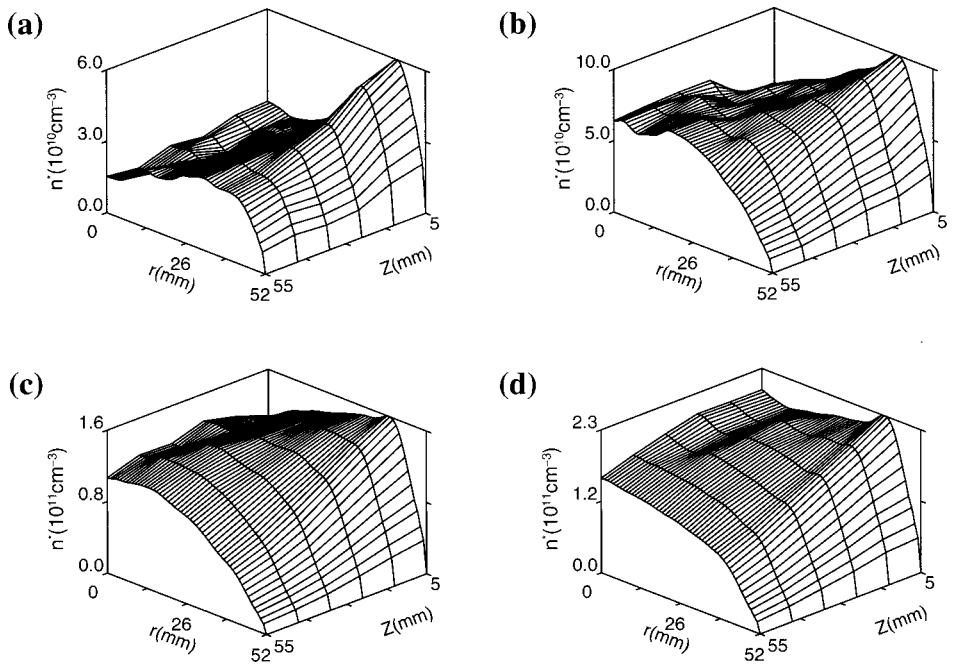

FIG. 2. Pressure dependence on two-dimensional spatial density distribution of the metastable ($1s_5$) for the ICP in pure argon for 100 sccm, 100 W, (a) 300 mTorr, (b) 100 mTorr, (c) 50 mTorr, and (d) 15 mTorr.

B. Power dependence of the metastable density

In Fig. 3 we show radial density distribution of metastables close to the coil plane ($z=5$ mm), as a function of power for two different pressures of 15 mTorr [Fig. 3(a)] and 300 mTorr [Fig. 3(b)]. Even for the lowest power of 20 W the highest density of metastables has been reached. In this case the profile is broad.

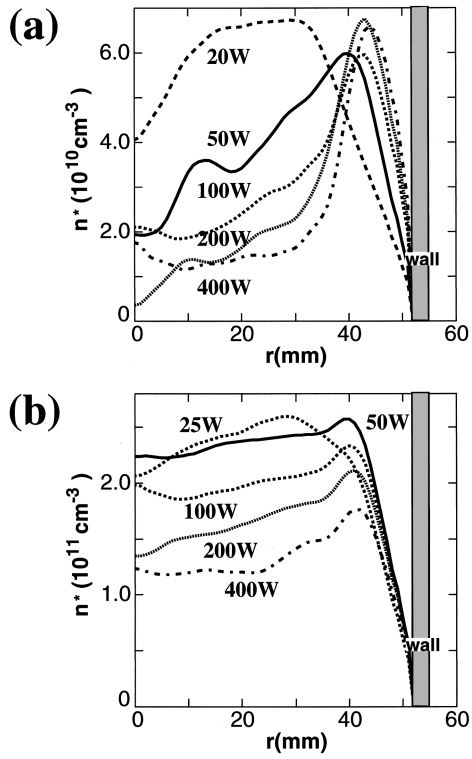

FIG. 3. Power dependence on radial density distribution of the metastable Ar($1s_5$) for the ICP in pure argon for 100 sccm, z= 5 mm, (a) 300 mTorr, (b) 15 mTorr.

The increase of the power brings the reduction of the density first in the center and then gradually towards the walls. This is more pronounced as the pressure increases. At 300 mTorr [Fig. 3(a)] at 400 W there is a sharp and narrow profile in the region of the expected high production rate close to the walls. The maximum of profile remains almost constant, regardless of the power, at the value of approximately 6×10^{10} cm^{-3}, only the position of the maximum slowly approaches the wall.

At 15 mTorr the behavior is somewhat different [Fig. 3(b)]. The profiles at the two lowest powers are almost identical. At the higher power of those two a maximum develops close to the walls but the overall value around 2.3×10^{10} cm^{-3} is achieved throughout the entire profile. As the power increases the mean density drops almost linearly both in the bulk of distribution and close to the wall. Gradually the peak close to the wall becomes more pronounced as the power increases. The position of the peak approaches the wall with the increasing power, the same as in the high-pressure situation.

The observed profiles may be understood on the basis of the following argument. For the higher pressure the excitation extends over the region of high azimuthal field. The field is shielded from the center of the discharge by the high concentration of charged particles. Increased power increases the density of charged particles, and the transition region where the azimuthal field may give energy to electrons is limited to the narrower and narrower region close to the walls. The field profile also has to be convoluted with the radial dependence of the electron number density, which is almost constant for this pressure (see Fig. 4).

At the lowest pressure covered here the azimuthal field does not extend deep into the discharge but as mentioned above electrons have long mean free paths and carry the high energy to the center. There are two possible explanations for the radial dependencies of metastable densities obtained at

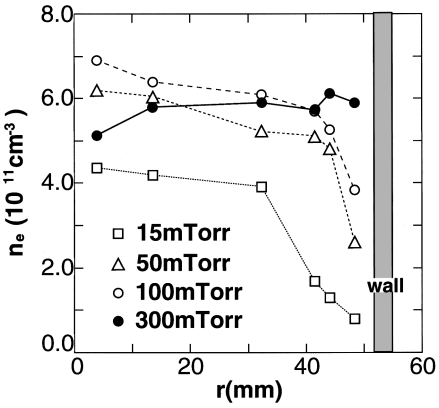

FIG. 4. Spatial density distribution of electrons in ICP in argon by using the Langmuir probe for 100 sccm, 100 W, and $z=5$ mm.

low pressure. The first is that the caldera shaped profile reflects the radial profile of electrons (see Fig. 4) where electron number density drops down rapidly for $r>32$ mm thus allowing the metastable maximum to occur at around 40 mm. The second is that the pressure is still sufficiently high to allow two different groups of electrons with different energies, one in the bulk and one in the azimuthal field region whereby the latter group, though with lower density, may have very high excitation rates due to the higher energy. This effect would have to be combined with the effect of electron induced quenching of metastables. The Monte Carlo simulations that are being performed will try to resolve which of the two possibilities is correct.

C. Comparison of the spatial profiles of radiative and metastable states

Comparison of radial profiles of metastables and radiative states can provide some general conclusions on the significance of the different loss processes. The effect of stepwise processes and of electron induced quenching on the plasma structure may be observed even better by comparing the spatial distribution of the metastable $1s_5$ with that of the excited state $3p_5$ for different powers as shown in Fig. 5 and Fig. 6. The data for two different pressures are shown, 15 mTorr in Fig. 5 and 300 mTorr in Fig. 6. Measurements were taken for different distances from the coil $z=5$, 25 and 45 mm.

When we consider the effect of stepwise process on plasma structure, we should especially give attention to the region where few high energy electrons exist, i.e., the center of the plasma. As shown in Figs. 5(a) and 5(b), at $z=5$ mm, i.e., the region near the coil, the number density of the excited state increases by a factor of 1.5 with power, while it increases by a factor of 2.0 at z= 45 mm. This is in contradiction to what may be expected if direct excitation dominates. On the other hand, as shown in Figs. 5(c) and 5(d), the number density of the metastables significantly decreases near the coil ($z=5$ mm) as power increases, but it changes much less in the region far from the coil ($z=45$ mm). In the region near the coil, the electron density increases with power. However, far from coil the increase of electron density with power may be expected only at low pressures where mean free paths are sufficiently long. The relative increase of the radiative excited state number density

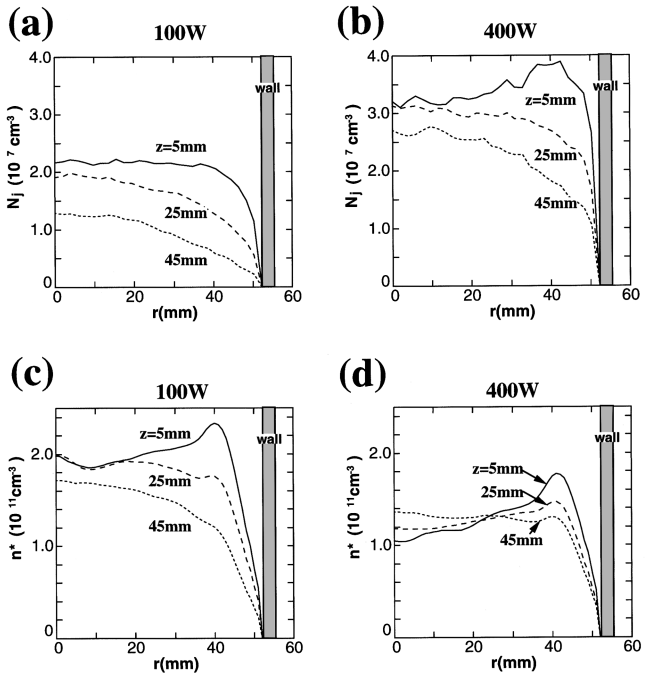

FIG. 5. Spatial density distribution of the excited state Ar($3p_5$) [(a) and (b)] and the metastable Ar($1s_5$) [(c) and (d)] in the ICP in argon. The distance from the coil is 5 mm, 25 mm, and 45 mm. The pressure is 15 mTorr. The power in (a) and (c) is 100 W, and in (b) and (d) is 400 W.

with power that is lower near the coil than far from the coil implies a reduced stepwise excitation due to metastable electron induced quenching. These results show that the plasma structure is affected by the spatial distribution of the meta-

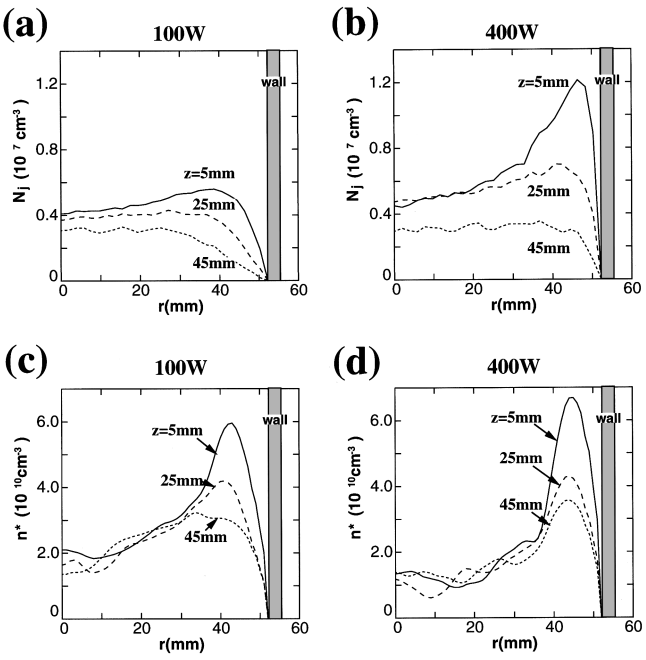

FIG. 6. Spatial density distribution of the excited state Ar($3p_5$) [(a) and (b)] and the metastable Ar($1s_5$) [(c) and (d)] in the ICP in argon. The distance from the coil is 5 mm, 25 mm, and 45 mm. The pressure is 300 mTorr. The power in (a) and (c) is 100 W, and in (b) and (d) is 400 W.

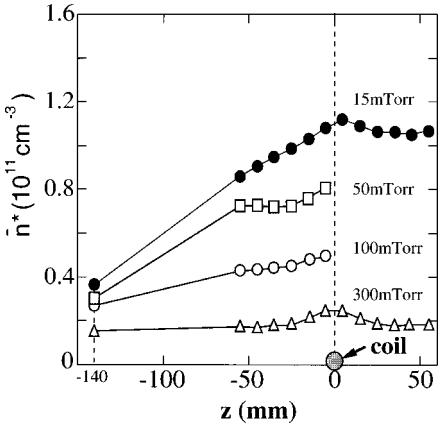

FIG. 7. Mean density distribution of the metastable Ar($1s_5$) in ICP in argon for 100 sccm and 400 W as a function of pressure.

stables even at lower pressure.

At the higher pressure of 300 mTorr (see Fig. 6) the high-energy electrons are less abundant over the entire radius. Thus the excitation process should more significantly depend on the stepwise processes by way of metastables. At the lower pressure (see Fig. 5) the number density of excited states increases with power over the entire radius even though metastable density decreases by almost a factor of 2. At the higher pressure the density of excited $3p_5$ states remains unaffected by the increase of power in the center of the discharge. The significant increase occurs close to the walls [Figs. 6(a) and 6(b)] As the density of metastables near the center also decreases almost by a factor of 2 [see Fig. 6(c)] with the increase of power, this implies a more pronounced stepwise excitation at the higher pressure. Close to the walls there is a small increase of the metastable density of the order of 10–20 % [see Fig. 6(d)] and consequently in this region the excited state density of $3p_5$ increases significantly with power.

D. Axial profile of metastables

Finally we show in Fig. 7, the axial density distribution of the metastable $1s_5$. Pressure was varied between 15 and 300 mTorr, while power was fixed at 400 W. The number density in Fig. 7 shows the mean density on the line through the origin ($r=0$ mm), and z corresponds to the distance from the coil. The coordinate $z=-140$ mm is the position, where the target is usually placed for remote processing, far from the plasma source. Unfortunately it was not possible to perform measurements in the gap between $z=-140$ mm and $z=-55$ mm due to obstructions from the flanges and walls of the chamber supporting the quartz cylinder.

At all pressures high metastable densities (an order of 10^{10} cm^{-3}) were obtained even at $z=-140$ mm. At this distance from the coil, where electrons are not expected to be present in significant numbers, only the diffusion of metastables in addition to the gas flow, can produce a significant population. At 15 mTorr the number density of the metastable linearly decreases while at the highest pressure of 300 mTorr it is almost constant. Loss of electrons due to electron induced quenching that dominates in the region of the coil will not affect the metastable density away from the coil.

At 15 mTorr an asymmetry in respect to $z=0$ mm can be seen. It is considered that this asymmetry is caused by the asymmetry in the axial profile of electron number density. Above the coil, there is a quartz wall at 95 mm above the coil. On the other hand, a distinct boundary in the axial direction exists only at 160 mm under the coil. Thus the density of electrons is not perfectly symmetric in respect to the $z=0$ plane giving rise to the profile that is slightly asymmetric especially at a distance of the order of $z=40$ mm away from the coil. Another possible explanation for the increase of metastable density near the top wall of the system may be due to reflection from the surface.

When observing these profiles we must bear in mind that we have plotted the density at the center of the discharge only. If the radial distribution of the metastables is quite pronounced as is the case at 300 mTorr the diffusion will merge these metastables from the region close to the wall into the central region at sufficiently large distances, especially when the loss due to electron induced quenching diminishes. Thus the axial dependence at high pressures reflects also the flux of numerous metastables from the regions close to the walls near the coil where significant production occurs. Thus its variation with z may be less pronounced. At low pressures the radial profile is almost constant.

IV. CONCLUSION

In this paper we have shown measurements of the metastable atom densities as a function of radial position in a single-coil ICP operating at 13.56 MHz. The results were presented as a function of distance from the coil, power, and pressure. One general feature is that the spatial profiles of the metastables that were observed are markedly different from the profiles of radiative states such as the $3p_5$ state. The differences come basically from the importance of the electron induced quenching in combination with a possible stepwise excitation of the higher radiative state. As a result of the electron induced quenching an increase in power does not necessarily increase the density of metastables, in fact, more often than not it decreases it. In addition there are two distinct regions with different behavior. In the center of the discharge where production is small, the effect of increased electron density is large and decrease of the metastable density with increasing power is strong. In the region close to the walls where significant electron heating occurs, the effect of increasing power is small; usually the peak value is not affected. This means that the number density of electrons, which may increase in this region as the power goes up, will be outweighed by the increased mean energy and therefore increased production rate. At lower pressures the distinction between the two regions is smaller or lost completely and here the decrease of the density with power occurs throughout the entire radius of the discharge.

Comparison of the radial dependencies of radiative and metastable state number densities gives information on the relative importance of stepwise excitation (and consequently ionization). Thus at higher pressures the stepwise effect is much more important and the power dependence of the density of the $3p_5$ state is weak due to the loss of metastables by increased electron quenching.

We should also note that the axial profiles of the meta-

stable density taken far from the coil have a high value even 140 mm from the coil. This is promising, since such profiles may be used as models for the transport of reactive radicals. The axial profiles are worthy of further analysis especially having in mind the value of the sticking and reflection coefficients for the particular particle and, also, studies at higher flow rates are also warranted.

Our data are in general agreement with the results of Hebner [3]. We both observe that the $1s_5$ state has a much higher density than $1s_3$. In addition, the power dependence was similar for the dominant metastable state and, also, Hebner finds a different spatial profile of the radiative $1s$ states. Spatial profiles cannot be easily compared due to a different geometry of the discharge and different overall conditions such as degree of anisotropy and axial dependence of the fields. In our case the studies that have been performed give a more systematic coverage of factors relevant for the conditions of our experiment and requirements of the theory. Our study was more directly aimed at analyzing the effect of metastables in stepwise processes and therefore more directly compared to the excitation profiles for radiative states. The spatial resolution in our system is higher and in all cases the data were converted to the metastable densities rather than line integrals.

In comparison between ICP and CCP the fact that the absolute densities of metastables are similar or only slightly higher in ICP may be misleading. [7] The kinetics of metastables is completely different. The two order of magnitude higher electron density in ICP gives a much higher production rates and also the loss rates. Other loss processes are small compared to electron induced quenching. For example adding small amounts of molecular gases would have less influence on the density of metastables in ICP because resonant excitation transfer would be a small loss process as compared to electron quenching [7]. At the same time the stepwise processes are much more important and it is possible to sustain the discharge even in the absence of the very-high-energy electrons. Of course this argument is less applicable at lower pressures.

Finally we stress once more the need for comparisons of absolute experimental data with accurate models as a necessary step in the development of detailed computer codes required for plasma processing tool development, i.e., the ''virtual factory'' [24]. In general our experimental results agree with the basic results of the theory [4] but further adjustments to the model are required before exact quantitative comparisons may be performed.

ACKNOWLEDGMENTS

This work was partially supported by Keio University Special Grant-in-Aid for Innovative and Collaborative Research Projects, and by the Association of Super Advanced Electronics Technologies (ASET). One of the authors (Z.Lj.P.) is grateful to Keio University and for a Monbusho Grant, and also to MNTRS for partial support under Project No. 01E03. The authors want to acknowledge useful discussions with Dr. Nadar Sadeghi on the application of the laser absorption spectroscopy and on the operation of diode lasers.

[1] J. Hopwood, Plasma Sources Sci. Technol. **1**, 109 (1992); J.Y. Choe, I.P. Herman, and V.M. Donnelly, J. Vac. Sci. Technol. A **15**, 3024 (1997).

[2] A. Okigawa, T. Makabe, T. Shibagaki, N. Nakano, Z.L. Petrović, T. Kogawa, A. Itoh, Jpn. J. Appl. Phys., Part 1 **35**, 1890 (1996).

[3] G.A. Hebner, J. Appl. Phys. **80**, 2624 (1996).

[4] K. Iyanagi, N. Nakano, and T. Makabe, in *Effect of Metastables on 2D rf Inductively Coupled Plasma in Ar by using RCT Model*, edited by S. Miyake, Proceedings of the 15th Symposium on Plasma Processing (Japan Society for Applied Physics, Hamamatsu, 1998), p. 198.

[5] J.V. Jovanović, S. Vrhovac, and Z.Lj. Petrović, in the *17th SPIG XVI Summer School and International Symposium on the Physics of Ionized Gases*, edited by B. Marinković and Z.Lj. Petrović (Institute of Physics, Belgrade, 1994), p. 61; I.Yu. Baranov, V.I. Demidov, and N.B. Kolokolov; Opt. Spectrosc. **51**, 1316 (1981); J.F. Behnke, H. Deutsch, and H. Scheibner, Beitr. Plasmaphys. **25**, 41 (1985); J. Bretagne, M. Capitelli, C. Gorse, and V. Puech, Europhys. Lett. **43**, 1179 (1987); C.M. Ferreira and A. Ricard, J. Appl. Phys. **54**, 2261 (1983); C.M. Ferreira, J. Loureiro, and A. Ricard, *ibid.* **57**, 82 (1985); H.A. Hyman, Phys. Rev. A **418**, 441 (1978); H.A. Hyman, *ibid.* **420**, 855 (1979); O. Judd, J. Appl. Phys. **47**, 5297 (1976).

[6] Z.Lj. Petrović, S. Bzenić, J. Jovanović, and S. Djurović, J. Phys. D **28**, 2287 (1995); D.P. Lymberopoulos and D.J. Economou, J. Appl. Phys. **73**, 3668 (1993); G. R. Schellar, R.A. Gottscho, D.B. Graves, and T. Intrator, *ibid.* **64**, 598 (1988).

[7] F. Tochikubo, Z.Lj. Petrović, S. Kakuta, N. Nakano, and T. Makabe, Jpn. J. Appl. Phys., Part 1 **33**, 4271 (1994).

[8] A. Okigawa, Z.Lj. Petrović, M. Tadokoro, T. Makabe, N. Nakano, and A. Itoh, Appl. Phys. Lett. **69**, 2644 (1996).

[9] A. Okigawa, M. Tadokoro, A. Itoh, N. Nakano, Z.Lj. Petrović, , and T. Makabe, Jpn. J. Appl. Phys., Part 1 **36**, 4605 (1997).

[10] M. Tadokoro, H. Hirata, N. Nakano, Z.Lj. Petrović, and T. Makabe, Phys. Rev. E **57**, 43 (1998).

[11] M. Tadakoro, A. Itoh, N. Nakano, Z.Lj. Petrovic, and T. Makabe, IEEE Trans. Plasma Sci. (special issue, to be published).

[12] K. Kondo, H. Kuroda, and T. Makabe, Appl. Phys. Lett. **65**, 31 (1994).

[13] K. Kondo, H. Kuroda, and T. Makabe, Jpn. J. Appl. Phys., Part 1 **33**, 4254 (1994).

[14] B.K. McMillin and M.R. Zachariah, J. Appl. Phys. **77**, 5538 (1995); B. K. McMillin and M.R. Zachariah, *ibid.* **79**, 77 (1996); S. Rauf and M.J. Kushner, *ibid.* **82**, 2805 (1997).

[15] G.A. Hebner, J. Appl. Phys. **80**, 3215 (1996); K.P. Giapis, N. Sadeghi, J. Margot, R.A. Gottscho, and T.C. JohnLee, *ibid.* **73**, 7188 (1993).

[16] J.M. de Regt, R.D. Tas, and J.A. van der Mullin, J. Phys. D **29**, 2404 (1996).

[17] M. Fadlallah, J.P. Booth, J. Derouard, N. Sadeghi, and P. Be-

lenguer, J. Appl. Phys. **79**, 8976 (1996).
[18] N. Beverini, G. Cicconi, G.L. Genovesi, and E. Piano, Plasma Sources Sci. Technol. **6**, 185 (1997).
[19] M.F. Dony, A. Ricard, M. Wautelet, J.P. Dauchot, and M. Hecq, J. Vac. Sci. Technol. A **15**, 1890 (1997).
[20] K. Dzierzega, K. Musiol, E.C. Benck, and J.R. Roberts, J. Appl. Phys. **80**, 3196 (1996).
[21] D.A. Edrich, R. McWilliams, and N.S. Wolf, Rev. Sci. Instrum. **67**, 2812 (1996).
[22] Z.Lj. Petrović, B. Bošković, A. Jelenak, and B. Tomčik, Thin Solid Films **304**, 136 (1997).
[23] U. Kortshagen and L.D. Tsendin, Appl. Phys. Lett. **65**, 1355 (1994); U. Kortshagen, N.D. Gibson, and J.J. Lawler, J. Phys. D **29**, 1223 (1996); G. Mumken and U. Kortshagen, J. Appl. Phys. **80**, 6639 (1996).
[24] M.J. Kushner, W.Z. Collison, M.J. Grapperhaus, J.P. Holland, and M.S. Barnes, J. Appl. Phys. **80**, 1337 (1996); P.L.G. Ventzek, M. Grapperhaus, and M.J. Kushner, J. Vac. Sci. Technol. B **12**, 3118 (1994); W.Z. Collison and M.J. Kushner, IEEE Trans. Plasma Sci. **24**, 135 (1994); P.L.G. Ventzek, R.J. Hoekstra, and M.J. Kushner, J. Vac. Sci. Technol. B **12**, 461 (1994); R.J. Hoekstra, M.J. Grapperhaus, and M.J. Kushner, J. Vac. Sci. Technol. A **15**, 1913 (1997).